Available online at BCREC website: https://bcrec.id

Bulletin of Chemical Reaction Engineering & Catalysis, 15 (2) 2020, 545-560

Research Article

Sodium Periodate as a Selective Oxidant for Diclofenac Sodium in Alkaline Medium: A Quantum Chemical Approach

Madhu Gupta[1]*, Amrita Srivastava[1], Sheila Srivastava[2]

[1]Department of Chemistry, University of Lucknow, Lucknow, Uttar Pradesh, India.
[2]Chemical Laboratories, Feroze Gandhi College, Raebareli, Uttar Pradesh, India.

Received: 15th April 2020; Revised: 4th July 2020; Accepted: 6th July 2020;
Available online: 30th July 2020; Published regularly: August 2020

Abstract

Diclofenac sodium is a well known anti-inflammatory drug. It has also been proclaimed to exhibit adverse effects on aquatic animals through sewage and waste water treatment plants. Kinetic and mechanistic studies of the novel oxidation of diclofenac sodium (DFS) by sodium periodate were discussed with an emphasis on structure and reactivity by using kinetic and computational approach. The proposed work had been studied in alkaline medium at 303 K and at a constant ionic strength of 0.60 mol.dm^{-3}. Formation of [2-(2,6-dicloro-phynylamino)-phenyl]-methanol as the oxidation product of DFS is confirmed with the help of structure elucidation. The active species of catalyst, oxidant and oxidation products were recognized by UV and IR spectral studies. Proton inventory studies in H_2O–D_2O mixtures had been shown the involvement of a single exchangeable proton of OH^- ion in the transition state. All quantum chemical calculations were executed at level of density functional theory (DFT) with B3LYP function using 6-31G (d,p) basis atomic set for the validation of structure, reaction and mechanism. Molecular orbital energies, nonlinear optical properties, bond length, bond angles, reactivity, electrophilic and nucleophilic regions were delineated. Influence of various reactants on rate of chemical reaction were also ascertained and elucidated spectro-photometrically. Activation parameters have been assessed using Arrhenius-Eyring plots. A suitable mechanism consistent with observed kinetic results had been implicated and rate law deduced.

Keywords: Kinetics; Oxidation; Diclofenac sodium; NaIO4; Os(VIII) catalysis; DFT

How to Cite: Gupta, M., Srivastava, A., Srivastava, S. (2020). Sodium Periodate as a Selective Oxidant for Diclofenac Sodium in Alkaline Medium: A Quantum Chemical Approach. *Bulletin of Chemical Reaction Engineering & Catalysis*, 15(2), 545-560 (doi:10.9767/bcrec.15.2.7555.545-560)

Permalink/DOI: https://doi.org/10.9767/bcrec.15.2.7555.545-560

1. Introduction

In a chemical reaction, if all reagents along with catalyst are in similar phase then reaction is regarded as homogenous. In such cases, catalysts are deliberated as solute in liquid reactants. Practically homogenous catalysis is more alluring, because it has a discriminating nature towards desired product formation. Hence, their mechanisms are more approachable than heterogeneous catalysis for detailed investigation. In latest years several platinum group metal ions, including Ru(III), Os(VIII), Ir(III), Rh(III), and Pd(II), were extensively used as catalysts due to their strong catalytic influences in a variety of reactions [1–2]. The role of osmium(VIII), as a catalyst in some redox reactions, had been re-

* Corresponding Author.
E-mail: guptamadhu30@rediffmail.com (M. Gupta)

viewed [3–4]. Sodium periodate, an inorganic salt comprises a periodate anion and sodium cation, which can also be referred as sodium salt of periodic acid. During oxidation it reduces to periodite as stable product [5–6]. When our investigation had been done without mercuric acetate then reaction mixtures approach to pale yellow color. This yellow color manifested the formation of molecule due to interaction of iodide ion in oxidant. Because of this parallel reaction, there is hindrance in main oxidation reaction. Hence, iodide ion has to be discharged to obstruct the formation of iodine molecule. Here, mercuric acetate is utilized as scavenger or trapping agent for iodide ion. When I^- comes in contact of mercuric acetate, it forms a complex $[Hg(I)_4]^{2-}$ and I^- get trapped in this complex. In this way parallel reaction gets discontinued with the help of mercuric acetate.

Diclofenac sodium (DFS), *i.e.* [*o*-[(2,6-dichlorophenyl) amino]phenyl] sodium acetate, pertains with the non-steroidal anti-inflammatory drugs. There is a necessity to proliferate a simple and economical method for the probation of DFS in pharmaceutical preparations. This drug belongs to non-steroidal anti-inflammatory drugs (NSAIDs). It has several applications in medical field like analgesic, antipyretic and anti-inflammatory [7]. Although it has been acknowledged for its efficient role relieving pain of inflammation and primary dysmenorrhea, anti-inflammatory action and inhibits prostaglandin synthesis, but its mode of action is still not known clearly. It has also been employed in treatment of osteoarthritis, rheumatoid arthritis and ankylosing spondylitis [8]. Because of its least solubility, commercially it exists in form its sodium salt.

On the basis of above results obtained after completion of reaction, we analyzed that pH value plays paramount role for reaction. The rate constants for slowest step and other equilibrium constants are helpful for elucidation of reaction mechanism. The mechanism elaborated is a consequence of all experimental data, spectral, kinetic and mechanistic studies. The negligible effect of ionic strength and dielectric constant shows that there is a reaction between neutral and charged species. The values of ΔH and ΔS favors given reactions. In all cases the negative value of ΔS shows that intermediate is more ordered then reactants [9]. For theoretical study all quantum chemical calculations were executed at level of density functional theory (DFT) with B3LYP function using 6-31G (d,p) basis atomic set for the validation of structure, reaction and mechanism. Polarizability and hyper-polarizabilities values have been calculated along with NLO and NBO computations of the product [10]. Global reactivity descriptors, like ionization potential, electron affinity, electronegativity, electrophilicity index and chemical potential, have been computed to predict the reactivity of the molecule. These DFT calculations also help in the interpretation of complex formed during experimental conditions [11–15].

So far, there was no report on the kinetics of DFS oxidation by alkaline sodium periodate in presence of Os(VIII) catalyst. Due to pharmaceutical importance of DFS and complexity of proposed reaction, a detailed study of this reaction becomes important. This study aims to check the reactivity of DFS towards sodium periodate in Os(VIII) catalyzed reaction and also elucidate the active species of catalyst and oxidant. With the help of kinetic and spectral results, we arrive at a suitable mechanism and also compute thermodynamic quantities for various steps. All the quantities and facts are further verified by using computational approach towards reaction. Hence we could compare theoretical and experimental data. The elucidation of mechanism allows chemistry to be interpreted, understood and predicted.

2. Materials and Methods

2.1 Kinetic Measurements

The progression of reaction was pursued iodometrically and also confirmed spectrophotometrically at various temperatures. It was authenticated that there was no significant interference from other species present in the reaction mixture at this condition. The reaction was observed to more than 85% completion of the reaction. The orders for various species were elucidated from the slopes of plots of log reaction rate versus log of respective concentrations of species. The rate constants were reproducible within ±5%. Regression analysis of experimental data to procure regression coefficient 'r' and the standard deviation 'S', of points from the regression line, was performed with the Origin 6.0 professional.

2.2 Computational Quantum-Chemical Methods

All calculations were performed using Gauss-View 5.0.8 software [16]. The geometries of the ground state were fully optimized using the most popular B3LYP method [17], applying 6-31-G (d,p) [18] of basis sets without symmetry constraints and using default convergence criteria. The optimized structure ob-

tained after this computational study is helpful to study various parameters of both reactants and products, like bond length, bond angles, dipole moment, optical properties, *etc*. The output file of optimized structure was further used to run the file of energy, NLO, NBO, *etc*. which were helpful to define UV, MESP, optical properties, bond order *etc*. for that particular substrate. The approximation of the equations of the polarizing continuum (IEEPCM) [19] was used to consider the influence of a bulk solution at the same level. The charge of atoms was calculated by the semi-empirical quantum-chemical method of Hückel [20].

3. Results and Discussions

3.1 Stoichiometry and Product Analysis

The results indicated 1:2 stoichiometry between substrate and oxidant. The oxidation product of DFS oxidation was extracted with ether and recrystallised with aqueous alcohol. Only one product, i.e. [2-(2,6-dichlorophenylamino)-phenyl]-methanol, was isolated with the help of preparative TLC and other separation technique and characterized by UV and FT-IR spectral studies. The product was further confirmed by its characteristic IR spectrum (Figure 1). The absence of a sharp band (peak) at 1695 cm^{-1} (due to the acidic carbonyl in DFS) confirms the nature of the product. Further, the secondary amine (–NH) group observed around 3387 cm^{-1} in DFS is retained in the product. All these observations proved the formation of [2-(2,6-dicloro-phynylamino)-phenyl]-methanol as the major product. For the confirmation of product, spectrophotometer is calibrated by using distilled water as solvent and then formation of [2-(2,6-dicloro-phynylamino)-phenyl]-methanol as the oxidation product of DFS was confirmed by the peak around 262 nm ultraviolet spectrum which was recorded in the region 200-900 nm on UV-visible Double-Beam Spectrophotometer (systronic-2203) instrument with methanol as a solvent. The reaction products do not undergo further oxidation under the existing kinetic conditions (Scheme 1).

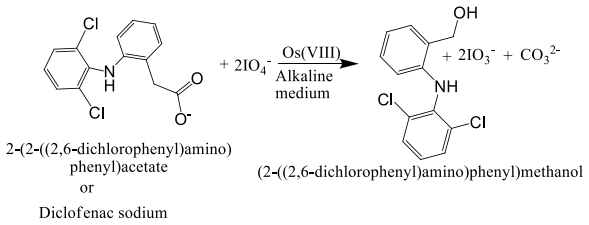

Scheme 1. Catalytic oxidation of diclofenac sodium

3.2 Kinetic Analysis

3.2.1 Reactivity of sodium periodate in alkaline medium

For determination of order of reaction with respect to sodium periodate at 35 °C in presence of Os(VIII) to oxidize diclofenac sodium by sodium periodate in alkaline medium various experiments were performed and the results are tabulated in Table 1. The concentration of [$NaIO_4$] varies from 0.83 ×10^{-3} to 5.00 × 10^{-3} M at constant concentration of other reactants. At fixed time (5 min.) rate of reaction for each kinetic run was determined by the slope of tangent. This Table 1 represents that rate of reaction is directly proportional to concentration of $NaIO_4$ which means increase in concentration of $NaIO_4$ also increases the rate of reaction. This first order kinetics is confirmed by linearity of the plot of log [$NaIO_4$] vs. log (–d*c*/d*t*) (*r* ≥

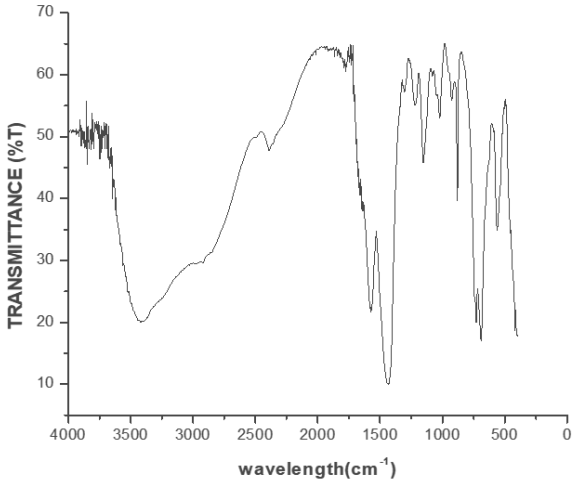

Figure 1. FT-IR spectrum of DFS oxidation product.

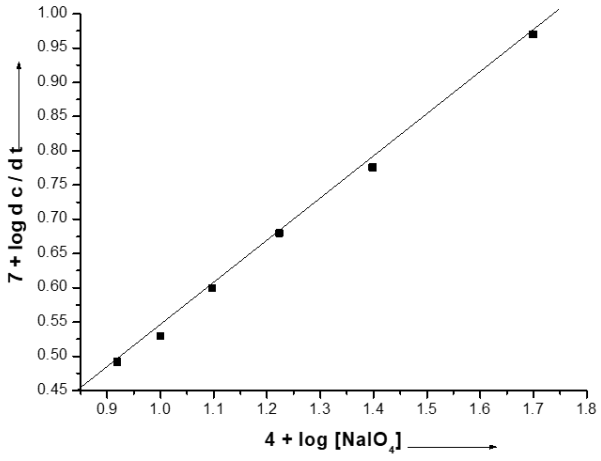

Figure 2. Plot of log [$NaIO_4$] vs. log (d*c*/d*t*) for oxidation of [DFS] at 35 °C.

0.99, $S \leq 0.062$) up to 85% completion of reaction (Figure 2). The first order kinetics is also supported by constant value of k_1 given in Table 1 and it was further confirmed by least square method (Figure 3).

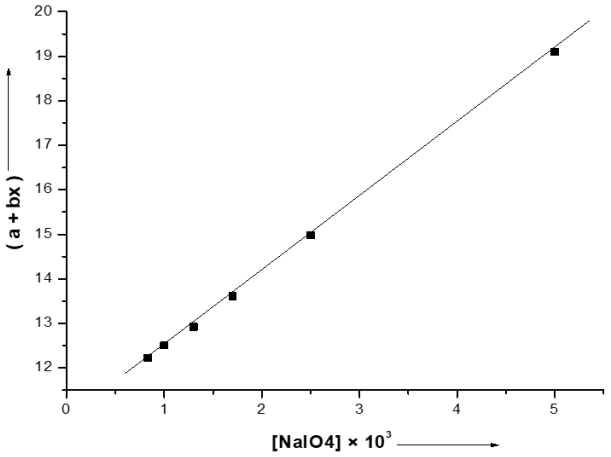

Figure 3. Plot of [$NaIO_4$] vs. (a+bx).

3.2.2 Effect of Osmium(VIII) Tetra Oxide

There are number of experiments which have been performed with different concentration of Os(VIII), while keeping concentration of other reactants constant at 35 °C, in order to

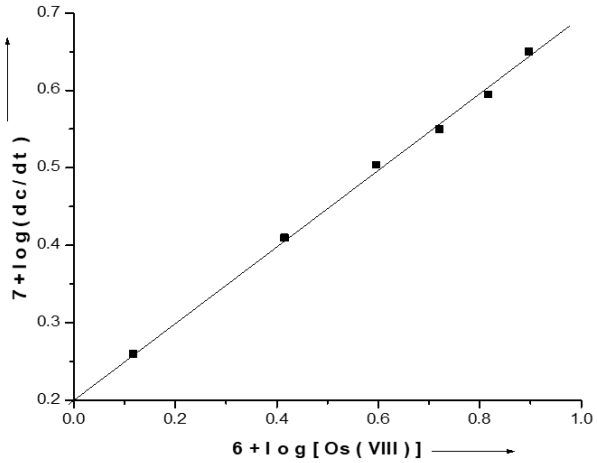

Figure 4. Plot of log[Os(VIII)] vs. log(dc/dt) for oxidation of DFS at 35 °C.

Table 1. Effect of Variation of [$NaIO_4$], [DFS], [OH^-], [IO_4^-] and [Os(VIII)] on the Osmium(VIII) Catalysed Oxidation of PAM by sodium periodate in Aqueous Alkaline Medium at 303 K and I = 0.005 mol.dm^{-3}

$[NaIO_4]\times10^3$ (mol.dm^{-3})	$[S]\times10^2$ (mol.dm^{-3})	Os(VIII)$\times10^{-6}$ (mol.dm^{-3})	$[NaOH]\times10^3$ (mol.dm^{-3})	$[Hg(OAc)_2]\times10^3$ (mol.dm^{-3})	$(-dc/dt)\times10^7$ (mol.dm^{-3}.s^{-1}) DFS	$k_1\times10^2$ (Observed)
0.83	1.00	2.6	1.00	1.25	3.10	4.13
1.00	1.00	2.6	1.00	1.25	3.20	4.05
1.25	1.00	2.6	1.00	1.25	3.24	4.00
1.67	1.00	2.6	1.00	1.25	4.32	4.17
2.50	1.00	2.6	1.00	1.25	5.32	4.16
5.00	1.00	2.6	1.00	1.25	9.82	4.23
1.00	1.00	1.31	1.00	1.25	1.60	2.11
1.00	1.00	3.94	1.00	1.25	2.49	4.53
1.00	1.00	5.25	1.00	1.25	2.70	5.29
1.00	1.00	6.56	1.00	1.25	3.40	6.67
1.00	1.00	7.88	1.00	1.25	3.60	8.18
1.00	0.13	2.6	1.00	1.25	2.10	2.82
1.00	0.17	2.6	1.00	1.25	2.20	2.97
1.00	0.25	2.6	1.00	1.25	2.31	3.07
1.00	0.50	2.6	1.00	1.25	2.30	3.19
1.00	2.00	2.6	1.00	1.25	2.40	3.48
1.00	1.00	2.6	0.83	1.25	3.30	5.40
1.00	1.00	2.6	1.25	1.25	2.80	4.38
1.00	1.00	2.6	1.67	1.25	2.70	4.50
1.00	1.00	2.6	2.50	1.25	2.60	3.61
1.00	1.00	2.6	5.00	1.25	2.40	2.79
1.00	1.00	2.6	1.00	0.83	4.00	4.65
1.00	1.00	2.6	1.00	1.00	4.30	4.83
1.00	1.00	2.6	1.00	1.67	3.20	3.33
1.00	1.00	2.6	1.00	2.50	3.14	4.36
1.00	1.00	2.6	1.00	5.00	2.75	3.49

determine the dependence of reaction concentration with respect to Os(VIII). The concentration of Os(VIII) ranges from 1.31×10^{-6} M to 7.88×10^{-6} M. The linear relationship between log [Os(VIII)] and log (-dc/dt) ($r \geq 0.99$, $S \leq 0.0021$) up to 85% completion of reaction (Figure 4). Figure 4 also shows that order of reaction is unity with respect to Os(VIII) throughout the reaction. These results are also confirmed by least square method (Figure 5).

3.2.3 Effect of alkaline medium

In case of oxidation of DFS, the reaction order with respect to [OH^-] is evaluated by various reaction experiments performed at 35 °C keeping all other reactants constant. The results of reaction are given in Table 1, in which sodium hydroxide concentration ranges from 0.83×10^{-3} M to 5.00×10^{-3} M, keeping constant concentration of other reactants. These results

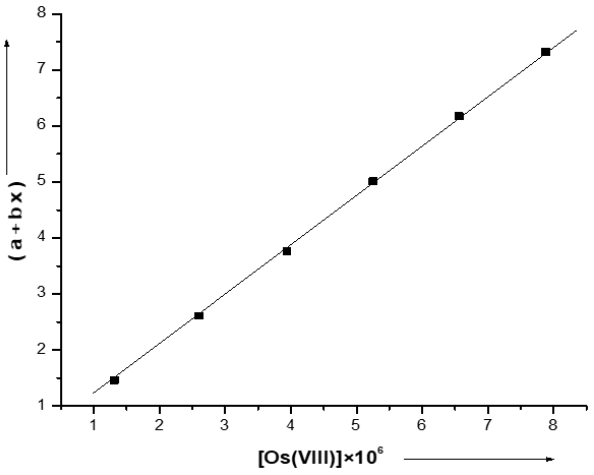

Figure 5. Plot between (a+bx) vs. [Os(VIII)]×10^6 for oxidation of DFS at 35 °C.

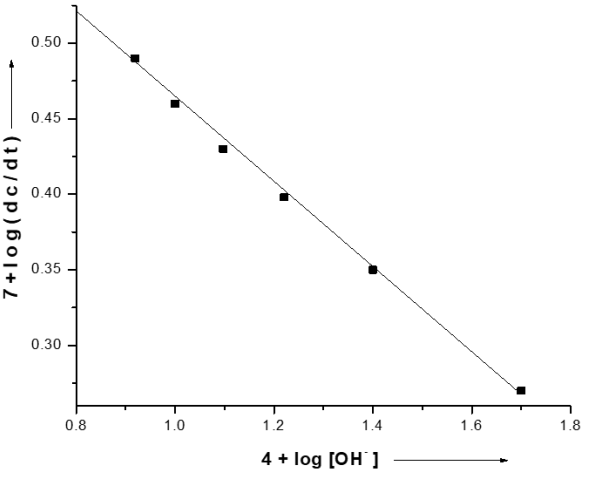

Figure 6. Plot of log [NaOH] vs. log (dc/dt) for oxidation of DFS at 35 °C.

may conclude that as the concentration of sodium hydroxide increases reaction rate decreases. Therefore reaction has negative effect with respect to hydroxide ion which is ascertained by the plot of log [NaOH] vs. log (−dc/dt) up to 90% completion of reaction (Figure 6).

3.2.4 Effect of substrate, heavy water addition, ionic strength, and dielectric constant

The effect of substrate was studied in the range of 0.13×10^{-2} to 2.0×10^{-2} mol.dm^{-3} at constant concentrations of $NaIO_4$, OH^-, IO_4^-, Os(VIII) and a constant ionic strength of 0.20 mol.dm^{-3}. The order with respect to [DFS] was fractional order. This was also justified by the plot of log dc/dt versus [DFS] ($r \geq 0.9979$, $S \leq 0.017$) (Figure 7). In alkaline medium different proportions of D_2O and H_2O have been used to study and determine the effect of addition of deuterium oxide (D_2O) in Os(VIII) catalyzed oxidation of pharmaceutical drugs (acetyl salicylic acid, acetaminophen and diclofenac sodium). The percentages of D_2O with H_2O in experiments are 0−100, 5−95, 10−90, and 20−80. The results of experiments are summarized no effect of heavy water on rate of reaction. So in order to justify current reaction mechanism we can say that there is no involvement of protonated reducing pharmaceutical drugs.

The ionic strength of any reaction provides the importance of Debye-Huckel limiting law and if the rate of reaction is proportional to concentration of activated complex then its validity is justified. Debye-Huckel gave the following equation to represent the relationship between activity coefficient and ionic strength-

$$\log_{10} k = \log_{10} k_0 + 1.02 Z_A Z_B \sqrt{\mu} \qquad (1)$$

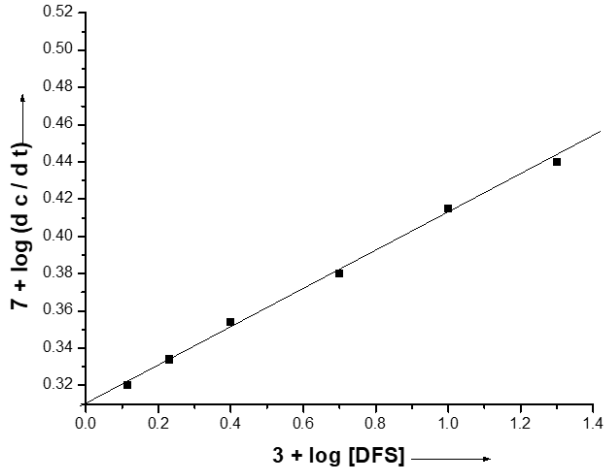

Figure 7. Plot of 3+log[DFS] vs. 7+log(dc/dt).

When the ionic strength varies in alkaline medium, this equation is reliable for measuring the rate of ionic reaction. A plot between $\log_{10}k$ versus $\sqrt{\mu}$ will give a straight line of slope $1.02Z_A.Z_B$. If the molecule is neutral, value of $Z_A.Z_B$ is zero then rate is independent of ionic strength. Alternatively, if $Z_A.Z_B$ is non-zero then ionic strength affects the rate of reaction. In our investigation we added $KClO_3$ in reaction mixture to elaborate the effect of ionic strength on reaction rate. In present investigation concentration of $KClO_3$ varies from 0.83×10^{-3} M to 5.00×10^{-3} M at constant concentration of all other reactants at 35 °C. The results prove that ionic strength has no effect on reaction rate and there is not certain alteration in d*c*/d*t* values.

3.3 Computational Details of Os(VIII) catalyzed oxidation of diclofenac sodium by sodium periodate in alkaline medium

3.3.1 Crystal Structure and Molecular Geometry

The calculated and experimental structure (Figure 8) of diclofenac sodium has longest distance between O29−Na30 is established to be 2.18 Å, due to interaction of carboxylate and sodium metal. The distance between C2−Cl22 and C4−C23 are 1.76 Å and 1.77 Å, respectively, because of interaction between lone pair of halogens and carbon atoms.

Due to the delocalization of nonbonding electrons from N10 to both phenyl rings the bond length between N10−H11 becomes shortest one, *i.e.* 1.01 Å. All C−C and C−H bond distances of rings are in the range 1.50-1.54 Å and 1.09-1.11 Å, respectively (Table 2). The symmetry of the molecule, with chloride substituent and N-substituted phenyl ring with a carboxylate ion, yields distortion in ring angles than 120°. The delocalization of non-bonding electrons of N10 results increase in bond angle (129.29°) than customary 120° while the C−O−Na has least bond angle, *i.e.* 87.24°.

Product was obtained as needle shaped crystal by slow evaporation of water solvent at room temperature and crystallized in triclinic system with space group C_1, with unit cell parameters a = 0.269287, b = 0.272785 and c = 0.443140. In product the computational calculated and experimental longest distance between C8−Cl14 and C12−Cl15 are 1.75 Å and 1.76 Å, respectively. Meanwhile, other C−C have bond length analogous to the experimental value (1.54 Å), and this was exactly similar for all C−C bonds and the smallest bond lengths are in between H28−O17, *i.e.* 0.9666 Å. Some bond angles C−N−C are above 120° due lone pair electrons of nitrogen atom. Other C−C−C are not much distorted from customary 120°. The resemblance between the optimized and experimental crystal structure is good enough displaying that the optimized structure is almost similar to the experimental structure. The existence of lone pair of electrons, electronegativity of the oxygen, nitrogen and chlorine atom causes distortion in bond angle and bond length.

3.3.2 Electronic absorption

Formation of [2-(2,6-dichlorophenylamino)-phenyl]-methanol as the oxidation product of diclofenac sodium was assured by the peak

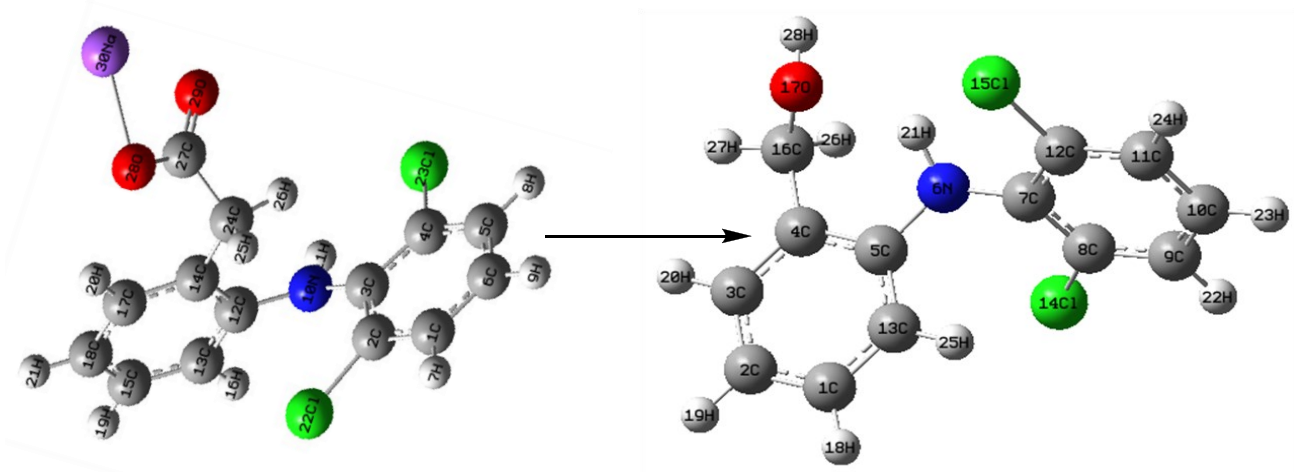

Figure 8. Optimized structure of reactant (Diclofenac sodium) and product ([2-(2,6-dichlorophenylamino)-phenyl]-methanol).

Sodium, Oxygen, Chlorine, Carbon, Hydrogen

Table 2. Comparison of bond length and bond angles of optimized structural parameters for diclofenac sodium and oxidation product, *i.e.* [2-(2,6-dichlorophenylamino)-phenyl]-methanol using B3LYP/6-31G (d,p) method.

Diclofenac sodium				Oxidation product			
Bond length (A°)		Bond Angle (°)		Bond length (A°)		Bond Angle (°)	
C2-C1	1.39316	C3-C2-C1	122.148	C2-C1	1.39417	C3-C2-C1	119.037
C3-C2	1.41621	C4-C3-C2	114.904	C3-C2	1.39519	C4-C3-C2	121.449
C4-C3	1.41904	C5-C4-C3	123.38	C4-C3	1.39538	C5-C4-C3	119.061
C5-C4	1.38794	C6-C1-C2	120.684	C5-C4	1.41343	N6-C5-C4	117.524
C6-C1	1.39149	H7-C1-C6	120.81	N6-C5	1.41046	C7-N6-C5	125.561
H7-C1	1.08413	H8-C5-C4	119.186	C7-N6	1.39382	C8-C7-C6	122.976
H8-C5	1.08394	H9-C6-C1	120.397	C8-C7	1.41389	C9-C8-C7	122.126
H9-C6	1.08445	N10-C6-C2	125.143	C9-C8	1.39286	C10-C9-C8	120.024
N10-C6	1.38186	H11-N10-C3	113.493	C10-C9	1.39266	C11-C10-C9	119.807
H11-N10	1.01061	C12-N10-C3	129.291	C11C10	1.3928	C12-C11-C10	119.493
C12-N10	1.43105	C13-C12-N10	116.492	C12-C11	1.39099	C13-C1-C2	120.613
C13-C12	1.40129	C14-C12-N10	123.171	C13-C1	1.39361	Cl14-C8-C7	119.983
C14-C12	1.41003	C15-C13-C12	120.967	Cl14-C8	1.754	Cl15-C12-C11	118.289
C15-C13	1.39058	H16-C13-C12	118.296	Cl15-C12	1.76025	C16-C4-C3	120.915
H16-C13	1.08584	C17-C14-C12	117.761	C16-C4	1.50455	O17-C16-C4	109.352
C17-C14	1.4034	C18-C17-C14	121.769	O17-C16	1.44008	H18-C1-C13	119.208
C18-C17	1.39265	H19-C15-C13	119.999	H18-C1	1.08624	H19-C2-C1	120.618
H19-C15	1.08605	H20-C17-C14	117.796	H19-C2	1.08528	H20-C3-C2	119.862
H20-C17	1.08532	H21-C18-C17	119.796	H20-C3	1.08718	H21-N6-C5	111.735
H21-C18	1.08639	Cl22-C2-C1	117.012	H21-N6	1.01668	H22-C9-C8	119.027
Cl22-C2	1.75829	Cl23-C4-C3	118.662	H22-C9	1.08391	H23-C10-C9	120.084
Cl23-C4	1.76758	C24-C14-C12	122.094	H23-C10	1.08484	H24-C11-C10	121.128
C24-C14	1.52052	H25-C24-C14	109.569	H24-C11	1.08384	H25-C13-C1	120.016
H25-C24	1.09658	H26-C24-C14	110.242	H25-C13	1.08448	H26-C16-C4	109.434
H26-C24	1.08901	C27-C24-C14	112.749	H26-C16	1.10096	H27-C16-C4	109.769
C27-C24	1.53417	O28-C27-C24	118.063	H27-C16	1.09812		
O28-C27	1.27441	O29-C27-C24	117.859				
O29-C27	1.26882			H28-O17	0.96665	H28-O17-C16	107.798
Na30-O29	2.18445	Na30-O29-C27	87.2435				

around 262 nm ultraviolet spectrum which was recorded in the region 200-900 nm on UV-visible Double-Beam Spectrophotometer (systronic-2203) instrument with water as a solvent. The UV-Visible spectrum of reactant and compound have been studied by TD-DFT method using B3LYP and 6-31-G (d,p) basis sets. The UV data with excitation energies, oscillator strength (*f*), percentage contribution of probable transitions and resultant absorption wavelengths have been analyzed with experimental results. The theoretical UV spectrum of DFS (*f*=0.0404) in water has an intense electronic transition at 224 nm and 272 nm while

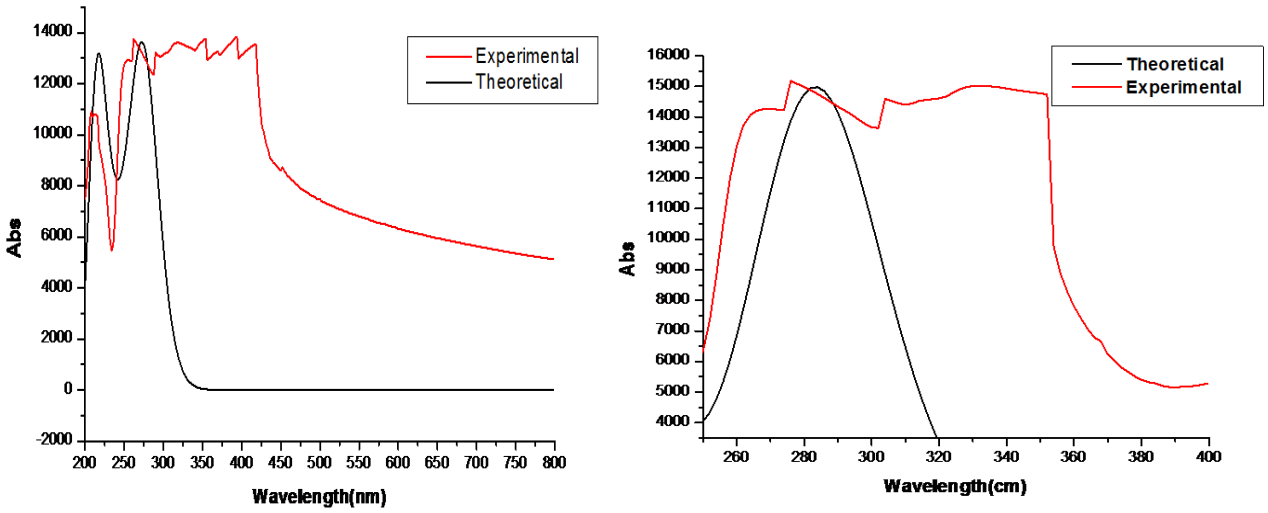

Figure 9. Experimental and theoretical UV-Visible spectrum of (a) diclofenac sodium (b) reaction product.

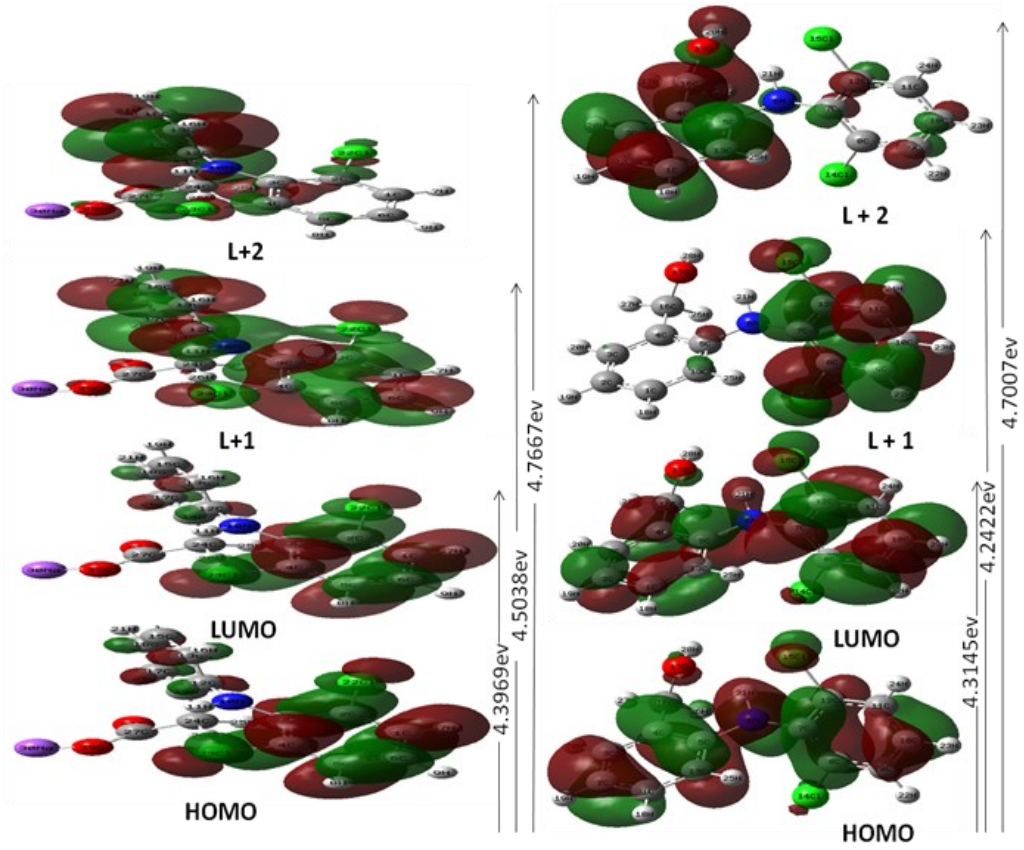

Figure 10. HOMO-LUMO transitions for diclofenac sodium and main product.

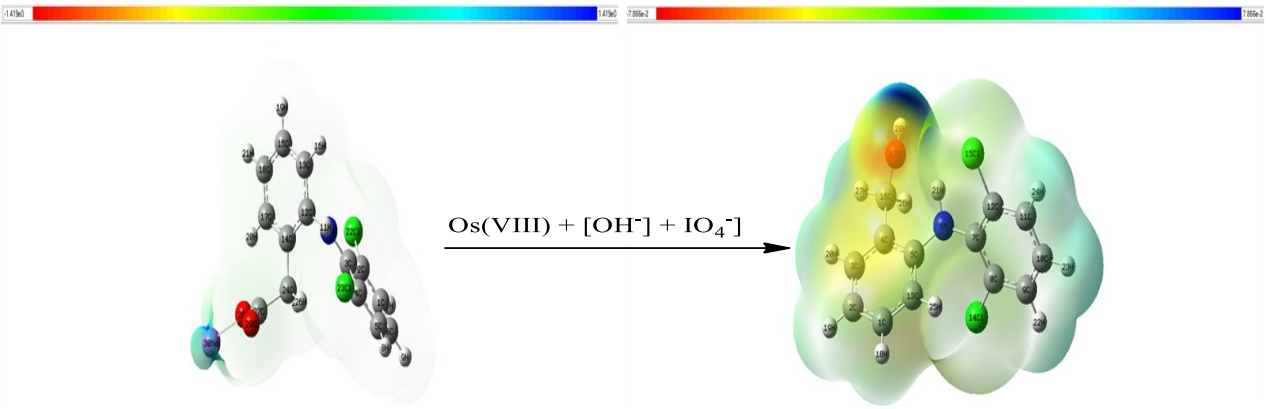

Figure 11. 3D plots of the molecular electrostatic potential of Diclofenacsodium and oxidation product.

Table 3. Second order perturbation theory analysis of Fock matrix in NBO basis of the [2-(2,6-dichlorophenylamino)- phenyl]-methanol as oxidation product.

Doner	Type	ED/e	Acceptor(j)	Type	ED/e	E(2)a	(Ej-Ei)b	Fij(c)
C1-C2	л	-0.24161	C3-C4	л*	1.67453	21.89	0.28	0.071
C1-C2	л	-0.24161	C5-C12	л*	1.67453	18.83	0.28	0.06
C3-C4	л	-0.24362	C1-C2	л*	1.68896	17.82	0.28	0.064
C3-C4	л	-0.24362	C5-C13	л*	1.68896	21.05	0.28	0.070
C16-O17	n	-0.24362	C3-C4	л*	1.68896	5.35	0.52	0.051
C5-C13	л	-0.24824	C1-C2	л*	1.64849	22.39	0.29	0.072
C5-C13	л	-0.24824	C3-C4	л*	1.64849	17.88	0.29	0.064
C7-C12	л	-0.24123	C8-C9	л*	1.66766	16.43	0.29	0.062
C7-C12	л	-0.24123	C10-C11	л*	1.66766	20.15	0.31	0.070
C8-C9	л	-0.27770	C7-C12	л*	1.70138	20.38	0.27	0.070
C8-C9	л	-0.27770	C10-C11	л*	1.70138	16.90	0.30	0.064
C10-C11	л	-0.25861	C7-C12	л*	1.65893	20.72	0.26	0.067
C10-C11	л	-0.25861	C8-C9	л*	1.65893	23.09	0.27	0.071
C7-C12	л	-0.00317	C8-C9	л*	0.45454	319.50	0.01	0.079
C7-C12	л	-0.00317	C10-C11	л*	0.45454	116.07	0.03	0.080
C8-C9	л	-0.00720	C10-C11	л*	0.00720	190.68	0.02	0.084
N6	n	-0.26182	C5-C13	л*	1.75295	27.44	0.30	0.083
N6	n	-0.26182	C7-C12	л*	1.75295	22.73	0.26	0.072
Cl14	n	-0.32645	C8-C9	л*	1.93103	11.38	0.33	0.060
Cl15	n	-0.33022	C7-C12	л*	1.93530	11.22	0.33	0.060
O17	n	-0.34483	N6-H21	σ*	1.94902	7.32	0.80	0.069
O17	n	-0.34483	C16-H27	σ*	1.94902	6.17	0.80	0.063

product (f=0.0111) has electronic transition at 286 nm, which complies with the measured experimental data of DFS (λ exp. = 262 nm and 288 nm) and product (λ exp. = 262nm and 318 nm), respectively (Figure 9).

These data corresponds to the transition from HOMO to LUMO with 64%, H to L+1 with 63% and H to L+2 transition with 63% contribution due to л → л* transition in diclofenac sodium . Product corresponds to the transition from HOMO to LUMO with 70%, H to L+1 with 69% and H to L+2 with 66% contribution due to л → л* transition (Figure 10). The given HOMO-LUMO of molecules represents the reactivity and kinetic sustainability their interaction. Since the energy gap between HOMO-LUMO least, so electron can be easily promoted from HOMO to LUMO. The molecular orbital diagram (Figure 10) shows that diclofenac sodium has more reactivity for proposed oxidation reaction.

3.3.3 Molecular electrostatic potential

The MEP value of diclofenac sodium around O_7 is −1.419 and MEP values of [2-(2,6-dichlorophenylamino)-phenyl]-methanol around −7.866 respectively. In oxidation product, C7, C12, and C11 is slightly electron rich in nature. The molecular electrostatic potential contour surface of diclofenac sodium and its oxidation product (Figure 11) shows that the negative regions are electrophilic regions, these are mainly over the oxygen atoms (O_{28}), while O_{29} is slightly electron deficient as MEP figure of diclofenac sodium depicted and O_{18} are slightly electron deficient in its oxidation product, the positive regions are the nucleophilic regions and these are over the carbon atoms connected with oxygen atom and over the hydrogen atoms of both the molecule. In both, the compounds chlorine atoms are neutral in nature while nitrogen atoms are electron deficient in nature.

3.3.4 Non-bond orbital analysis

NBO analysis has been performed on the molecule at the DFT/B3LYP/6-31G+ (d,p) level in order to elucidate the intramolecular and delocalization of electron density within the molecule, which are presented in Table 3. For oxidation product, C7−C12 of the NBO conjugated with л* (C8-C9) leads to an enormous stabilization of 319.50 kJ/mol. This strong stabilization denotes the larger delocalization. As the interaction around the ring increases the biological activity in the compound also enhanced. Second–order perturbation theory analysis of the Fock matrix in NBO basis for product is given in Table 3 and the correlation between donor (i), acceptor (j) and stabilization energy E(2) is given as:

$$E(2) = \Delta E_{ij} = q_i \frac{(F_{ij})^2}{\left(E_i - E_j\right)} \quad (2)$$

where qi = donor orbital occupancy, E_i and E_j = diagonal elements, and F_{ij} = off diagonal NBO fock matrix element. The NBO analysis represents the intramolecular charge transfer in product as:

Table 4. Calculated Dipole moment (μ_0), Polarizability ($|\alpha_0|$), First Hyperpolarizability (β_0) and their components, using B3LYP/6–31G(d,p)

Dipole moment			Polarizability			Hyperpolarizability		
Diclofenac sodium		Oxidation product	Diclofenac sodium		Oxidation product	Diclofenac sodium		Oxidation product
μ_x	-5.626	1.1057	α_{XX}	253.232	302.689	β_{XXX}	-339.05	755.059
μ_Y	-4.5268	0.3489	α_{XY}	-66.269	4.51117	β_{XXY}	-322.17	-303.68
μ_Z	0.1938	-1.481	α_{YY}	258.671	226.481	β_{XYY}	-42.042	130.073
μ	7.2237	1.8808	α_{XZ}	-11.371	12.1885	β_{YYY}	-174.51	-119.62
			α_{YZ}	0.8846	-11.855	β_{XXZ}	-289.68	384.164
			α_{ZZ}	224.271	145.387	β_{XYZ}	108.711	189.092
			α_0	36.367	33.3231	β_{YYZ}	371.866	-71.439
						β_{XZZ}	245.308	-119.03
						β_{YZZ}	-57.9	27.3989
						β_{ZZZ}	-351.32	-39.24
						β_{TOTAL} (esu)	5.453	7.81577

μ_0 in Debye; $|\alpha_0|$ and $\Delta\alpha$ in 10^{-24}esu; β_0 in 10^{-30}esu,

- From bonding л(C1-C2) to antibonding π* (C3-C4) and (C5-C13) with stabilization energy 21.89 kcal.mol^{-1} and 18.83 kcal.mol^{-1}.
- From bonding л(C3-C4) to antibonding π* (C1-C2) and (C5-C13) with stabilization energy 17.82 kcal.mol^{-1} and 21.05 kcal.mol^{-1}.
- From bonding n(C16-O17) to antibonding π* (C3-C4) with stabilization energy 5.35 kcal.mol^{-1}.
- From bonding л(C5-C13) to antibonding π* (C1-C2) and (C3-C4) with stabilization energy 22.39 kcal.mol^{-1} and 17.88 kcal.mol^{-1}.
- From bonding л(C7-C12) to antibonding π* (C8-C9) and (C10-C11) with stabilization energy 16.43 kcal.mol^{-1} and 20.15 kcal.mol^{-1}.
- From bonding л(C8-C9) to antibonding π* (C7-C12) and (C10-C11) with stabilization energy 20.38 kcal.mol^{-1} and 16.90 kcal.mol^{-1}.
- From bonding л(C10-C11) to antibonding π* (C7-C12) and (C8-C9) with stabilization energy 20.72 kcal.mol^{-1} and 23.09 kcal.mol^{-1}.
- From bonding л(C7-C12) to antibonding π* (C8-C9) and (C10-C11) with stabilization energy 319.50 kcal.mol^{-1} and 116.07 kcal.mol^{-1}.
- From bonding л(C8-C9) to antibonding π* (C10-C11) with stabilization energy 190.68 kcal.mol^{-1}.
- From LP (1) of N6 to л* (C5-C13) and (C7-C12) with stabilization energy of 27.44 kcal.mol^{-1} and 22.73 kcal.mol^{-1}.
- From LP (3) of Cl14 to л* (C8-C9) with stabilization energy of 11.38 kcal mol^{-1}.
- From LP (3) of Cl15 to л* (C7-C12) with stabilization energy of 11.22 kcal.mol^{-1}.
- From LP (2) of O17 to σ* (N6-H21) and (C16-H27) with stabilization energy of 7.32 kcal.mol^{-1} and 6.17 kcal.mol^{-1} originating due to corresponding delocalized movement of electrons inside the ring. The interaction between donor and acceptor also increases with the increase in value of E (2).

3.3.5 Non-linear optical analysis

The dipole moment of diclofenac sodium is 7.22D which is much higher than product (*i.e.* 1.88D), while the calculated polarizability and hyper polarizability of diclofenac sodium are 36.37×10^{-24} esu and 5.453×10^{-30} esu, respec-

Table 5. Calculated thermodynamic parameters of Diclofenac sodium and Oxidation product.

Parameters	B3LYP/6-31 G(d,p)	
Molecule	Diclofenac sodium	Oxidation product
Zero Point Vibrational Energy (kcal.mol^{-1})	132.29731	133.22198
Rotational Temperature (K)	0.1573	0.02531
	0.00960	0.01472
	0.00793	0.01127
Rotational Constant (GHz)		
X	0.32769	0.52734
Y	0.1999	0.30669
Z	0.16515	0.23481
Total Energy E_{total} (kcal.mol^{-1})	143.902	142.641
Translational	0.8890	0.889
Rotational	0.8890	0.889
Vibrational	142.125	140.863

Table 6. Calculated ε_{LUMO}, ε_{HOMO}, energy band gap $\varepsilon_{HOMO}-\varepsilon_{LUMO}$, ionization potential (IP), electron affinity (EA), electronegativity (χ), global hardness (η), chemical potential (μ), global electrophilicity index (ω), global softness (S) and additional electronic charge (ΔN_{max}) in eV for assayed compounds, using DFT/B3LYP/6-31G(d,p).

Name of compound	ε_H	ε_L	ε_H-ε_L	*IP*	*EA*	χ	η	μ	ω	S	ΔN_{max}
Diclofenac sodium	-5.7499	-0.581	5.169	5.75	0.58	3.165	2.585	-3.165	1.938	0.19	1.225
Product	-5.680	-0.688	5.113	5.680	0.688	3.184	2.496	-3.184	2.031	0.20	1.276

tively (Table 4). The values for both diclofenac sodium and its oxidation product were found to be greater than those of urea (the β_0 of urea 0.3728×10^{-30} esu). Thus, both are good NLO material.

3.3.6 Thermodynamic analysis

Due to the various chemical and physical phenomena thermodynamic analysis play consequential role in elucidation of reaction mechanism. In present analysis, we calculate zero point vibrational energy, rotational constants and various energies, using DFt-B3LYP/6-31G (d,p) method (Table 5). All the thermodynamic calculations are conducted in gas phase and not in solution.

3.3.7 Global reactivity descriptors

The global reactivity descriptors define the type of interaction, bonding and active centre of molecule which helps in elucidation of mechanism. The nature of molecular orbital defines its most reactive position while the HOMO-LUMO energy gap defines biological activity of that compound. Least energy gap indicates higher polarizability of molecule and less kinetic stability. Ionization potential (IP), electron affinity (E_A), electronegativity (χ), chemical potential (μ), global hardness (η), global softness (S), and electrophilicity index (ω) were listed in Table 6. As the HOMO-LUMO energy gap increases, the molecule becomes harder, which resist the deformation of electron cloud. The higher the value of the electrophilicity index (ω), the better is the electrophilic character. Hence, DFS is less electrophilic than its oxidation product.

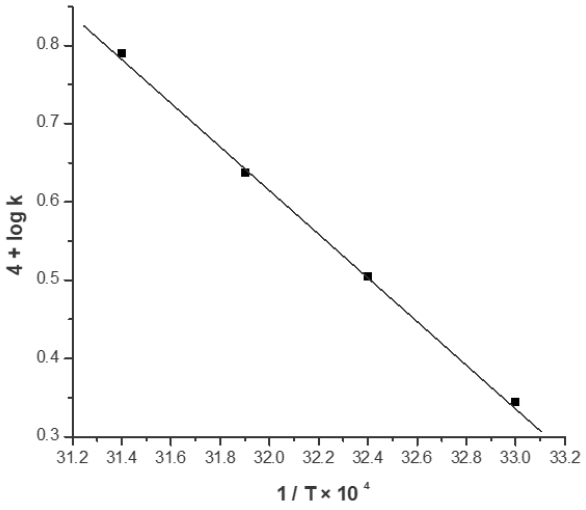

Figure 12. Arrhenius plot between log k vs. $1/T$ for oxidation of pharmaceutical drugs (acetylsalicylic acid, acetaminophen and diclofenac sodium).

3.4 Thermodynamic Analysis

A vant Hoff's plot was inclined for the variation of k with temperature [*i.e.* log k versus $1/T$] (Figure 12) and the values of the enthalpy of reaction ΔH, entropy of reaction ΔS, and free energy of reaction ΔG were calculated. Moderate ΔH^* and ΔE^* values are favourable for electron transfer reaction. Entropy of activation plays vital role in the chemical reaction between ions or between an ion and a neutral molecule or a neutral molecule forming ions. When reaction takes place between two ions of opposite charges, their union will results in a lowering of net charge, and due this some frozen solvent molecules will released with an increase of entropy. But on the other hand, when reaction takes place between two similarly charged species, the transition state will be a more highly charged ion, and due to this, more solvent molecules will be required for separate the ions, leading to a decrease in entropy. High positive value of free energy change of activation (ΔG^*) indicated that the transition state was highly solvated, while negative value of entropy of activation (ΔS^*) suggested the formation of an activated complex with reduction in degree of freedom. Deviation in the rate within the reaction series may be caused by change in the enthalpy or entropy of activation. A negative value of ΔS^* suggests that the two ionic species combine in rate determining step to give a single intermediate complex which is more ordered than the reactants [16−18].

Table 7. Thermodynamic activation parameters for the oxidation of DFS by sodium periodate catalysed by Osmium(VIII) in alkaline medium.

Temperature (K)	$k_1\times10^4$ (sec^{-1})	log A	9.53
303	2.94	Ea/($kJ.mol^{-1}$)	53.22
308	4.05	$\Delta H^{\#}$/($kJ.mol^{-1}$)	50.66
313	5.70	$\Delta S^{\#}$/($JK^{-1}.mol^{-1}$)	-66.52
315	8.20	$\Delta G^{\#}$/($KJ.mol^{-1}$)	20.54

3.5 Theory and Discussion of Results

Ionic strength determination accurately defines pH of solutions by estimating concentration of all ions in the solution. Similarly in any ionic reaction the interaction between ions play vital role because ions act like conducting spheres for solvent with constant dielectric constant (∈). According to Bohr model for ion in solutions, the force acting between ions,

$$f = -\frac{Z_A Z_B e^2}{4\pi \in_0 \in x^2} dx \tag{3}$$

The negative sign is used because x decreases by dx when ion moves together by a distance dx. The work executed for moving ions from its initial state to final d_{AB} is therefore,

$$w = -\int_{\infty}^{d_{AB}} \frac{Z_A Z_B e^2}{4\pi \in_0 \in x^2} dx = -\frac{Z_A Z_B e^2}{4\pi \in_0 \in d_{AB}} \tag{4}$$

If ions have same sign then work is positive otherwise vice versa. By using Gibbs free energy equation, Equation (4) may be written as,

$$\ln k = \ln k_0 - \frac{Z_A Z_B e^2}{4\pi \in_0 \in d_{AB} k_B T} \tag{5}$$

The slope of the line obtained by plotting ln k against $1/\in$ gives the value of $Z_A Z_B e^2 / 4\pi \in_0 d_{AB} k_B T$. Hence, we can calculate d_{AB} from experimental slope. For elaborating the effect of dielectric constant, we use various ratios of Acetic acid and water percentage which alters the dielectric constant of the medium (D). The D values were deliberated from the equation,

$$D = D_W V_W + D_A V_A \tag{6}$$

where D_W and D_A are the dielectric constants of pure water and acetic acid respectively and V_A and V_B are the volume of fractions of components, water and acetic acid, respectively in total mixture. Different reactions were performed with various concentration of acetic acid keeping concentration of all other reactants constant at 35 °C. The concentration of acetic acid varies from 5% to 20% (v/v). The results emphasize that there was no significant effect of dielectric constant under the experimental conditions.

The low value of rate constant for slow step of the mechanism confirms that the oxidation apparently occurs through an inner-sphere mechanism. This conclusion was supported by previous literature [19–20]. The catalyst Os(VIII) forms the complex with organic substrates, which enhances the reducing ability of the substrate than that with no catalyst. Further, the catalyst Os(VIII) modifies the reaction pathway by lowering the energy of activation. The Os(VIII) catalyzed reaction, however, is logically fast in view of speediness of Os(VIII) to act across the –COO bond. The reaction product does not manipulate the rate in alkaline media since it has been observed that it is not involved in the pre-equilibrium process. All of the observations also confirm the proposed mechanism. On the basis of kinetic results, active species of Os(VIII) oxide and sodium periodate and other kinetic properties with respect to [Substrate], [OH^-], [Hg(II)] and ionic strength of medium, the following mechanistic steps are proposed.

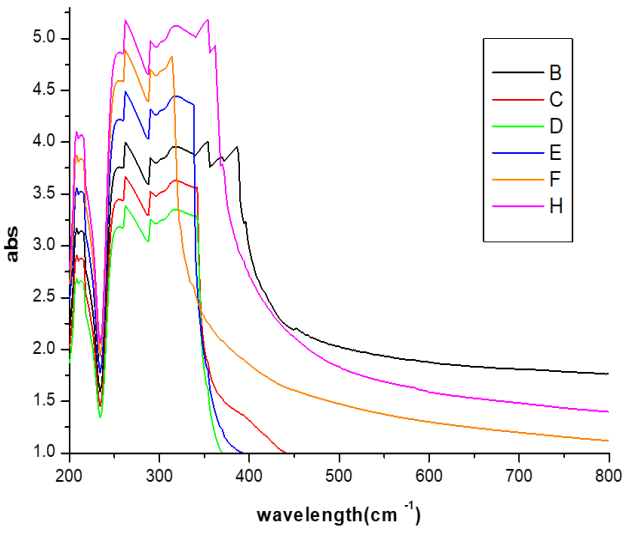

Figure 13. UV spectra showing effect of alkali, oxidant, DFS and catalyst for Os(VIII) catalysed oxidation of DFS by sodium periodate at 35 °C.

3.6 Reaction Mechanism

The negative effect of [OH-] indicates that in above reaction equilibrium shifted towards right (Scheme 2). Therefore, the [OsO4(OH)2]- is the active species of osmium(VIII) oxide in alkaline medium.

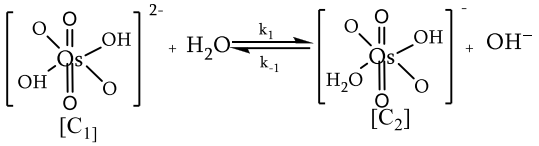

Scheme 2: Hydrolysis of hydrated osmium tetra oxide

Now in view of above mechanistic steps (Scheme 3), the steady state approximation is applied and following rate law is derived. [Os(VIII)$_T$] is equal to sum of concentration of,

$$\frac{d\left[IO_4^-\right]}{dt} = rate = k_3\left[IO_4^-\right][Complex]$$

$$Rate = \left\{\frac{k_3K_1K_2\left[IO_4^-\right][Os(VIII)_T][Drugs]}{1+K_1+\left[OH^-\right]}\right\} \quad (7)$$

The rate law is in agreement with all observed kinetics.

According to mechanism proposed above, Os(VIII) forms complex with drugs. This complex increases the reducing property of substrates and decreases the energy of activation for reaction. The oxygen atom of carboxyl group of the ASA is involved in the formation of intermediate, as the molecular order in ASA. The drugs react with active species of osmium tetra oxide to give a complex, which further reacts with one mole of sodium periodate in rate determining slow step with regeneration of catalyst. Then reaction undergoes a fast step to consume another mole of oxidant, which provides main product of reaction. The probable structure of the complex [C$_3$] formed in oxidation reactions are given in Scheme 4.

The spectroscopic evidence for formation of complex between catalyst and substrate was obtained from UV-Vis spectra of drug (1.0×10^{-2} mol.dm^{-3}), Os(VIII) (2.6×10^{-6} mol.dm^{-3}), [OH$^-$] (1.0×10^{-3} mol.dm^{-3}) and mixture of both (Figure 13). A hypsochromic shift in between drug and mixture of Os(VIII) was observed.

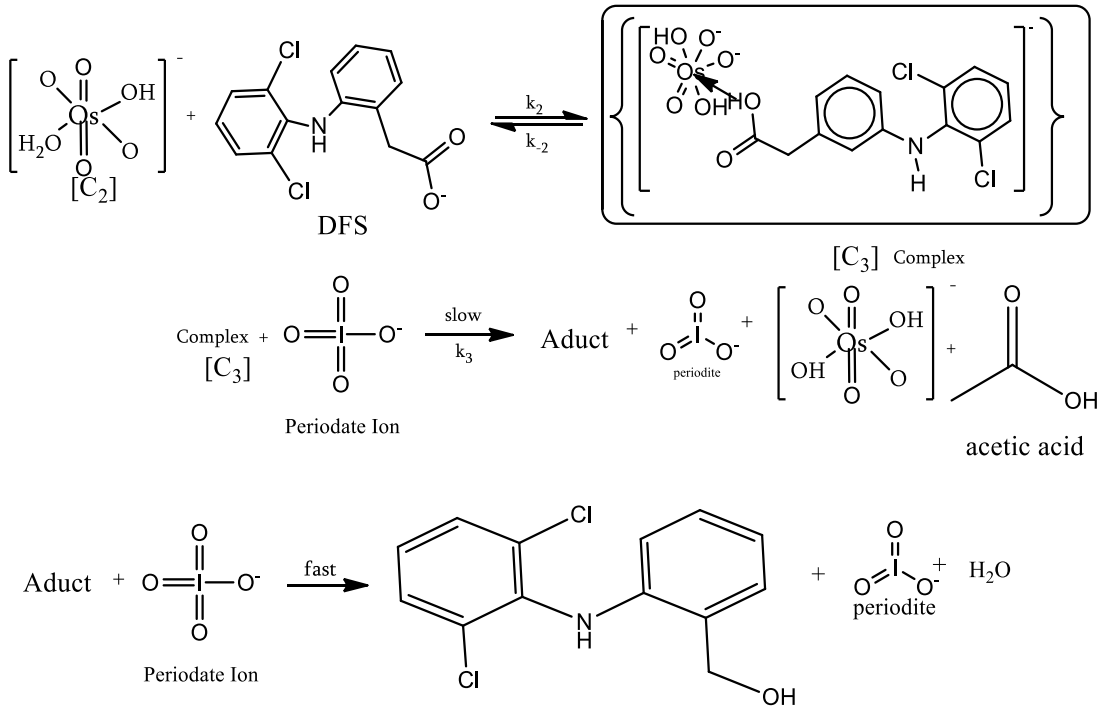

Scheme 3. Reaction mechanism of product formation

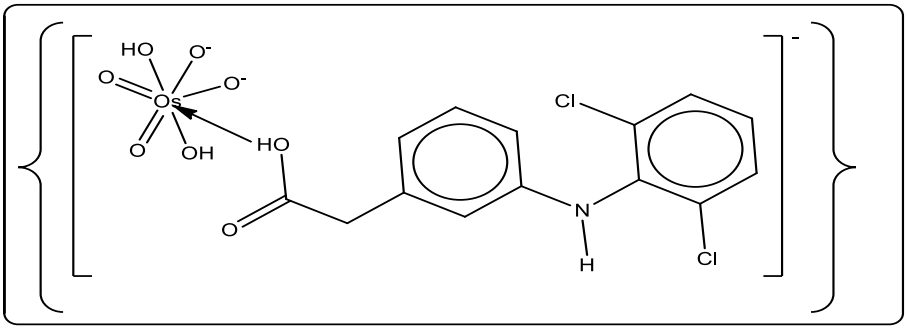

Scheme 4: Structure of complex formed during DFS oxidation

The Lineweaver-Burk plot proved the complex formation between Os(VIII) and drug, which explains fractional order in [drug]. The rate law for Scheme 1 is derived as,

$$Rate = \frac{d\left[IO_4^-\right]}{dt}$$

$$Rate = \left\{\frac{k_3 K_1 K_2 \left[IO_4^-\right]\left[Os(VIII)_T\right]\left[Drugs\right]}{1 + K_1 + \left[OH^-\right]}\right\} \quad (8)$$

$$k = \frac{Rate}{\left[IO_4^-\right]} = \left\{\frac{k_3 K_1 K_2 \left[Os(VIII)_T\right]\left[Drugs\right]}{1 + \left[OH^-\right] + K_1}\right\} \quad (9)$$

The rate law (9) can be rearranged to Equation (10), which is suitable for verification. Equation (10) proves that the plots of [Os(VIII)]/k vs. 1/[drug] and [Os(VIII)]/k vs. [OH$^-$] were linear (Figure 14).

$$\frac{\left[Os(VIII)_T\right]}{k} = \frac{1}{k_3 K_1 K_2 \left[Drugs\right]} + \frac{\left[OH^-\right]}{k_3 K_1 K_2 \left[Drugs\right]} + \frac{1}{k_3 K_2 \left[Drugs\right]} \quad (10)$$

4. Conclusion

The oxidation of DFS by NaIO4 experienced a slow reaction rate in alkaline media, but increased in rate in the existence of the Os(VIII) catalyst. The observed results were explained by plausible mechanisms and the related rate laws were deduced which were further justified by the application of computational approach. The catalyst Os(VIII) forms complex with DFS, which shows a great reducing property than DFS itself. In the absence of catalyst oxidation of DFS by NaIO4 is very lethargic, but it becomes superficial in the presence of Os(VIII) catalyst. The reactive species of NaIO4 is IO_4^- not NaIO4 itself. Oxidation products were recognized and activation parameters were evaluated. The observed results have been explained by a reasonable mechanism and the related rate law. The observed results have been explained by mechanism and related law has been deduced. Since the HOMO–LUMO energy gap of product is lower than DFS, so that the product is less stable. On basis of NLO calculations value of βo for both DFS and product were higher than urea so both have good optical property. Therefore, we can conclude that both plays vital role in pharmaceutical industry and have NLO applications.

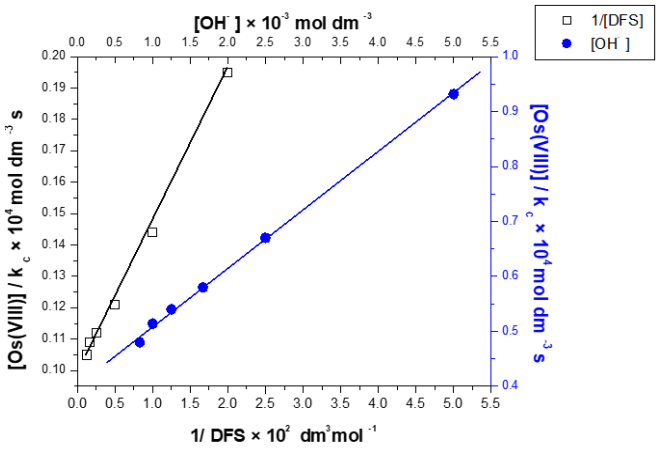

Figure 14. Verification of rate law (2) in form of (3) for Os(VIII) catalyzed oxidation of DFS by sodium periodate at 35 °C.

Acknowledgements

The authors convey their profound thanks to the Head, Department of Chemistry, Lucknow University, Lucknow, for providing laboratory facilities for spectral analysis and central facility for computational research. Authors wish to thank reviewers for greatly improving the paper.

References

[1] Srivastava, S., Gupta, M. (2015). Osmium(VIII) Catalysed Oxidation of Leucine by Alkaline Sodium Periodate: A Kinetic Study. *Bulletin of Catalysis Society of India,* 14(1), 1-5.

[2] Gupta, M., Srivastava, A., Srivastava, S. (2018). Kinetic Mechanistic, and Thermodynamic Studies for Oxidation of L-Alanine by Alkaline Sodium Periodate in Presence of Os(VIII) in its Nano Concentration Range as Homogenous Catalyst. *Bulletin of Chemical Reaction Engineering & Catalysis*, 13(2), 355-364. DOI: 10.9767/bcrec.13.2.1583.355-364.

[3] Iliescu, T., Baia, M., Miclaus V.A. (2004). A Raman spectroscopic study of the diclofenac sodium–ß-cyclodextrin interaction. *European Journal Pharmaceutical Science,* 22(5), 487-495. DOI: 0.1016/j.ejps.2004.05.003.

[4] Gostick, N., James, I.G., Khong, T.K., Roy, P., Shepherd, P.R., Miller, A.J. (1990). Controlled-release indomethacin and sustained-release diclofenac sodium in the treatment of osteoarthritis: A comparative controlled clinical trial in general practice. *Current Medical Res. Opin.*, 12(3), 135-142. DOI: 10.1185/03007999009111494

[5] Griffith, W. (1967). *The Chemistry of Rarer Platinum Metals*. Wiley-Interscience Publishers: New York, pp. 141.

[6] Rassolov. V., Ratner, M., Pople, J. (2001). 6-31G* basis set for third-row atoms. *J. Comp. Chem.*, 22, 976-984. DOI: 10.1002/jcc.1058.

[7] Hugar, G.H., Nandibewoor, S.T. (1994). Kinetics of osmium(VIII) catalysis of periodate oxidation of DMF in aqueous alkaline medium. *Transition Metal Chemistry*, 19, 215-217. DOI: 10.1007/BF00161893.

[8] Singh, A., Singh, S.P., Singh, A.K., Singh, B. (2007). Mechanistic study of palladium(II) catalysed oxidationof crotonic acid by periodate in aqueous perchloric acid medium. *Journal of Molecular Catalysis A*, 266, 226-232. DOI: 10.1016/j.molcata.2006.10.046.

[9] Srivastava, A., Gupta, M., Srivastava, S. (2019). Kinetic, Spectroscopic and DFT Studies of Novel Oxidation of Acetylsalicylic Acid by NaIO4 using Micro-amount of Os(VIII) as a Homogeneous Catalyst in Alkaline Medium *Russian Journal of Physical Chemistry A*, 93(10), 2031-2039 DOI: 10.1134/S0036024419100297.

[10] Gupta, M., Srivastava, A., Srivastava, S. (2019). Comparative Study of Kinetic and Mechanistic Study of Oxidation of L-Alanine and L-Proline by Sodium Periodate Catalyzed by Osmium(VIII) in Micromolar Concentrations, *Russian Journal of Physical Chemistry A*, 93(1), 48-58. DOI: 10.1134/S0036024419010096.

[11] Farhat, M.F., El-Saghier, A.M.M., Makhlouf, M.A., Kreddan, K.M., Elmezoughi, A.B. (2007). Ketene *N*,*S*-acetals in heterocyclic synthesis: part 1: synthesis of *N*-phenyl-2-ylidene and 2,5-diylidene-4-thiazolidinone derivatives. *Journal of Sulfur Chemistry,* 28, 563–572. DOI: 10.1080/17415990701586823

[12] Barakat, A., Soliman, S.M., Al-Majid, A.M., Lotfy, G., Ghabbour, H.A., Fun, H.K., Yousuf S., Choudhary, M.I., Wadood, A. (2015). Synthesis and structure investigation of novel pyrimidine-2,4,6-trione derivatives of highly potential biological activity as anti-diabetic agent. *Journal of Molecular Structure*, 1098, 365–376. DOI: 10.1016/j.molstruc.2015.06.037

[13] Naseem, S., Khalid, M., Tahir, M.N., Halim, M.A., Braga, A.A.C., Naseer, M.M., Shafiq, Z. (2017). Synthesis, structural, DFT studies, docking and antibacterial activity of a xanthene based hydrazone ligand. *Journal of Molecular Structure,* 1143, 235–244. DOI: 10.1016/j.molstruc.2017.04.093

[14] Sakka, O.K., Fleita, D.H., Harrison, W.T.A. (2013). 2-(4-Oxo-3-phenyl-1,3-thiazolidin- 2-ylidene)malononitrile. *ActaCrystallogr. E. Struct. Rep. Online*, 69, 350. DOI: 10.1107/s160053681300216x

[15] Ahmad, M.S., Khalid, M., Shaheen, M.A., Tahir, M.N., Khan, M.U., Braga, A.A.C., Shad, H.A. (2018). Synthesis and XRD, FT-IR vibrational, UV–vis, and nonlinear optical exploration of novel tetra substituted imidazole derivatives: a synergistic experimental-computational analysis. *J. Phys. Chem. Solids*, 115, 265–276. DOI: 10.1016/j.jpcs.2017.12.054

[16] Frisch, Æ., Gaussian 09WReference, Gaussian, Inc., Wallingford, CT, 2009.

[17] Frisch, M.J., Trucks, G.W. et al., Gaussian 09, Revision A.02, Gaussian, Inc., Wallingford CT, 2016.

[18] Tirado-Rives, J., Jorgensen, W. (2008). Performance of B3LYP Density Functional Methods for a Large Set of Organic Molecules. *Journal of Chemical Theory Computational*, 4, 297-306. DOI: 10.1021/ct700248k.

[19] Caricato, M. (2012). Exploring Potential Energy Surfaces of Electronic Excited States in Solution with the EOM-CCSD-PCM Method. *Journal of Chemical Theory Computational,* 8, 4494-4502. DOI: 10.1021/ct300382a.

[20] Pyykko, P., Laaksonen, L. (1984). Relativistically parameterized extended Hueckel calculations. 8. Double-.zeta. parameters for the actinoids thorium, protactinium, uranium, neptunium, plutonium, and americium and an application on uranyl. *Journal of Physical Chemistry*, 88, 4892-4895. DOI: 10.1021/j150665a017.

[21] Sethuram, B. (2003). Some Aspects of Electron Transfer Reactions Involving Organic Molecules, Allied Publishers (P) Ltd., Mumbai, India.

[22] Laidler, J.K. (2004). Chemical Kinetics, 3rd ed.; Pearson Education Ptc. Ltd.: New Delhi, India.

[23] Upadhyay, S.k., Agrawal, M.C. (1977). Kinetics of os(viii)-catalysed alkaline hexacyanoferrate (iii) oxidation of some alpha -amino acids in presence of excess of ferrocyanide. *Indian Journal of Chemistry*, *15a*, 709.

[24] Sutin, N. (1966). The kinetics of inorganic reactions in solution. *Annual Review of Physical Chemistry*, 17, 119–172.

[25] Lancaster, M., Murray, R.S. (1971). Ferricyanide-Sulphite Reaction, *Journal of Chemical Society*, A, 2755-2755-2758. DOI: 10.1039/J19710002755